Fe_3O_4 Nanocrystals with Novel Fractal

Guifu Zou, Kan Xiong, Changlong Jiang, Hui Li, Tanwei Li, Jin Du, and Yitai Qian*

Hefei National Laboratory for Physical Science at Microscale and Department of Chemistry, University of Science and Technology of China, Hefei, Anhui 230026, P. R. China

Received: May 22, 2005; In Final Form: July 8, 2005

Fe_3O_4 novel fractal nanocrystals have been synthesized by a surfactant-assisted solvothermal process for the first time. X-ray diffraction (XRD), X-ray photoelectron spectra (XPS), Mössbauer spectroscopy (MS), scanning electron microscopy (SEM), and transmission electron microscopy (TEM) have been used to investigate the novel fractal nanocrystals. The lengths of the fractals are about 2−3 μm, and the trunks and branches of Fe_3O_4 fractals have almost the same diameters of ca. 30−50 nm. The roles of surfactant PEG-20000 and N_2H_4 have been discussed in detail. One key fact has been found that the ferrocene concentration has a vital effect on the morphologies of the products. The side-branching process and the oscillation of the concentration have been proposed to illustrate the formation mechanisms of the fractal nanocrystals. In addition, magnetic properties of Fe_3O_4 fractal nanocrystals have also been detected by a vibrating sample magnetometer, showing relatively high saturation magnetization (***Ms***) of ca. 78.75 emu/g.

Introduction

During the past decades nanostructured materials have attracted considerable attention due to their fundamental significance for physical properties and potential application in nanodevices.[1] Much effort has been made to study their novel physical properties (such as electronic, magnetic, and optical traits) as well as the quantum confinement effect and space-confined transport phenomena, differing from those of their bulk materials.[2] It is well known that the properties of nanomaterials are affected not only by their chemical composition, but also by their structure, shape, and size.[3] Moreover, the architectural design for nanomaterial shapes is critical for building of 'bottom-up' approaches toward future nanodevices. Among nanomaterials with different structures, one-dimensional (1D) nanoscale materials[4] have stimulated great interest due to their unique properties, providing an ideal model system to experimentally investigate physical phenomena.[5] Recently, one novel fractal structure of 1D nanoscale materials has been also attracting much attention, and fractal nanocrystals have recently been more focused due to their nonequilibrium growth.[6] Variable related phenomena have been found and investigated in chemical systems, especially fractal patterns, which have shown a new nonlinearly scientific world and may provide a geometry method to describe the nature morphology.[7,8] To date, some fractal nanocrystals have been observed.[9] Although nanomaterials with different morphologies have been prepared, selective synthesis of the novel nanoscale morphologies always turns out to be a great challenge to material scientists.

Nanoscale magnetic materials have attracted much attention as the materials in this size ring would allow investigating the fundamental aspects of magnetic-ordering phenomena in magnetic materials with reduced dimensions and could also lead to new potential applications such as high-density recording media, magnetic sensors, etc.[10] Magnetite (Fe_3O_4), an important member of spinel-type ferrite, is used widely as a pigment,[11] recording material,[12] electrophotographic developer, and catalyst,[13] etc. Many methods have been reported for the synthesis of the Fe_3O_4 nanoparticles, such as microwave hydrothermal synthesis, reduction of hematite Fe_2O_3 by CO or H_2, oxidation of the ferrous hydroxide gels using KNO_3, γ-ray radiation, and discharge.[14] If the magnetic nanoparticles can be grown into 1D or complex fractal nanocrystals, it may greatly improve their magnetism and widen their other potential uses. Unfortunately, this successful synthesis has not been realized due to the spinel structure and inherent magnetism of Fe_3O_4.[15] To the best of our knowledge, there have been no reports about magnetic Fe_3O_4 fractal nanocrystals. In this study a surfactant-assisted solvothermal process has been developed to synthesize Fe_3O_4 fractal nanocrystals for the first time. The growth mechanism has been properly proposed to discuss the fractal nanocrystals formations.

Experimental Section

All chemicals used in this work, such as ferrocene ($Fe(C_5H_5)_2$), acetone (C_3H_6O), hydrazine hydrate ($N_2H_4{\cdot}H_2O$, 50%), and poly(ethylene glycol)-20000 (PEG-20000), are A. R. regents from the Shanghai Chemical Factory, China. $Fe(C_5H_5)_2$ (0.186 g, 2 mmol) and PEG-20000 (2.000 g) were added to 30 mL of C_3H_6O and stirred to form a homogeneous solution. Then 10 mL of $N_2H_4{\cdot}H_2O$ was added to the solution and stirred for 2 min. Finally, the mixture was transferred into a Teflon-lined autoclave of 60 mL capacity. The autoclave was filled with C_3H_6O to 80% of the total volume, sealed, and maintained at 240 °C for 20 h. Afterward the autoclave was allowed to cool to room temperature naturally. The products were collected and washed several times with acetone, deionized water, and absolute ethanol and then dried in a vacuum oven at 40 °C for 4 h. The final black powders were obtained, and the yield of Fe_3O_4 nanocrystals with novel fractals is about 90% for many of the experimental observations.

Characterization. The X-ray diffraction (XRD) are performed on a Rigaku (Japan) D/max-γA X-ray diffractionmeter equipped with graphite-monochromatized Cu Kα radiation (λ =1.5418 Å). X-ray photoelectron spectra (XPS) are recorded on a VGESCALABMK X-ray photoelectron spectrometer using nonmonochromated Mg Kα radiation as the excitation source. The binding energies obtained in the XPS analysis are standard-

10.1021/jp052678c CCC: $30.25
Published on Web 09/08/2005

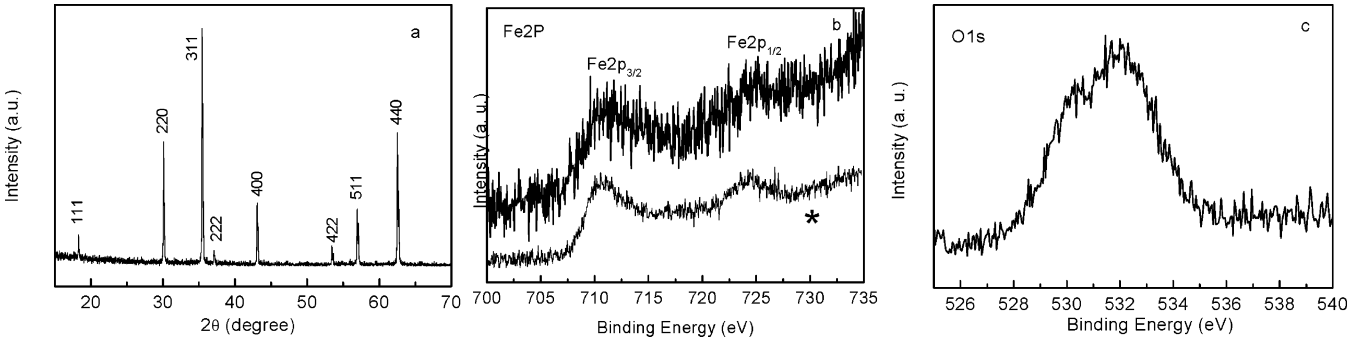

Figure 1. (a) XRD pattern of the Fe_3O_4 fractal nanocrystals. (b and c) XPS spectrum of as-obtained Fe_3O_4 fractal nanocrystals (the asterisk (*) curve indicates the Fe 2p peak of the Fe_3O_4 commercial powders).

ized for specimen charging using C1s as the reference at 284.6 eV. The Mössbauer spectrum (MS) is recorded on a MS-404 V4.04 Spectrometer with a ^{57}Co source in a Pd matrix on a constant acceleration drive at room temperature and zero fields, and hyperfine interaction parameters are derived from the use of a Newton−Gauss method. The scanning electron microscopy (SEM) images are taken on a field emission scanning electron microscope (JEOL JSM-6300F, 15 KV). The transmission electron microscopy (TEM) images and the corresponding selected-area electron diffraction (SAED) patterns are taken on a JEOL 2010 high-resolution transmission electron microscope at an acceleration voltage of 200 KV. Magnetic hysteresis loops are measured using a vibrating sample magnetometer (VSM, BHV-55). For magnetization measurements the powder is pressed strongly and fixed in a small cylindrical plastic box.

Results and Discussion

Figure 1 shows the XRD pattern of Fe_3O_4 fractal nanocrystals obtained in the experiments. All peaks can be indexed as face-centered cubic Fe_3O_4 with lattice constant $a = 8.391$ Å, which is very close to the reported data (JCPDS 85-1436, $a = 8.393$ Å). No characteristic peaks of impurities can be detected. The strong and sharp reflection peaks suggest that the as-prepared fractal nanocrystals are well crystallized. The fractal nanocrystals obtained are further examined by X-ray photoelectron spectra (XPS). Their spectra are shown in Figure 1b and c, corresponding to the binding energies of Fe2p and O1s. The Figures show that the binding energies corresponding to $Fe2p_{3/2}$, $Fe2p_{1/2}$, and O1s are ca. 710, 723, and 532 eV, respectively. Compared with the Fe2p peak of the Fe_3O_4 commercial powders (asterisk curve shown in Figure 1b), their corresponding values are almost identical. The data are also consistent with the reported values of Fe_3O_4 in the literature,[16] and XPS results prove the composition of the products. To further ascertain the phase of the iron oxides, the Mössbauer spectrum of the products has been measured, and the results are shown in Figure 2. The hyperfine parameters can be obtained to be 49.0 and 45.9 T (hyperfine field) and 0.11 and 0.49 mm/s (isomer shift), corresponding to Fe^{3+} ions at sites A and (Fe^{2+}, Fe^{3+}) ions at site B, respectively. These results agree well with those reported for the Fe_3O_4 nanoparticles.[10a,17] The acute and strong lines of the magnetic sextets suggest that the obtained Fe_3O_4 products are crystalline. Therefore, the pure phases of Fe_3O_4 fractal nanocrystals with crystallinity can be obtained in the experimental processes.

The morphology of the products is examined by SEM. Figure 3a is a typical SEM image of the products, clearly showing that Fe_3O_4 possesses a novel fractal structure. Examining numerous SEM images of the samples, we find that almost all nanocrystals have this kind of fractal structure. After further studying the higher magnification SEM image (shown in Figure

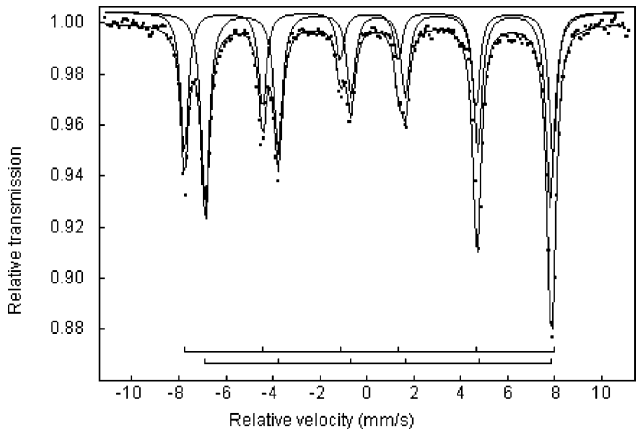

Figure 2. Mössbauer spectrum of the Fe_3O_4 fractal nanocrystals measured at room temperature.

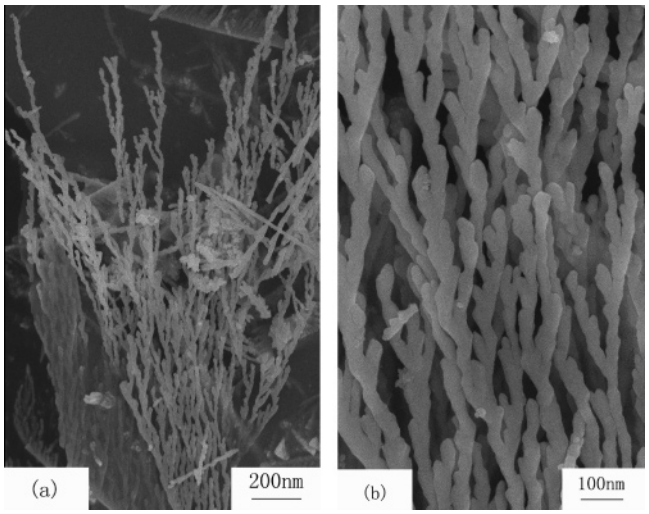

Figure 3. Low-magnification (a) and high-magnification (b) SEM images of the Fe_3O_4 fractal nanocrystals.

3b) some interesting phenomena can be seen. First, the individual Fe_3O_4 fractal only has branches on the two-dimensional (2D) plane, not in three-dimensional (3D) space. Second, although the fractals have no regular shape, every branch of the fractals has almost same structure. Third, every branch has the forward growth trend. It might be related to the inherent magnetic property of Fe_3O_4. The lengths of the fractals are about 2−3 μm, and the trunks and branches of Fe_3O_4 fractals have almost same diameters of ca. 30−50 nm. Besides the fractal nanocrystals, some Fe_3O_4 nanoparticles can be found in the products also. The structural characterizations of the fractal nanocrystals were also investigated in detail by TEM, SAED, and high-resolution TEM (Figure 4). Figure 4a shows the TEM

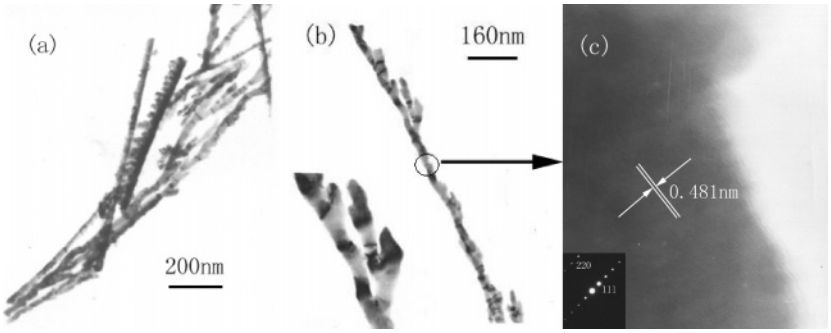

Figure 4. TEM images of the products (a) and one fractal nanocrystal (b). (inset b) High-magnification TEM image of the fractal branches. (c) High-resolution TEM image of the fractal. (inset c) The corresponding SAED pattern.

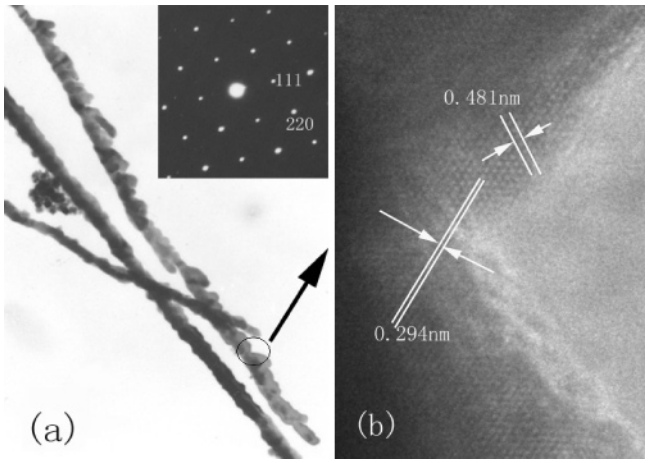

Figure 5. TEM images of the products (a). (inset a) SAED pattern of the junction of the trunk and branch. (b) High-resolution TEM image of the junction.

image of the products. We find that many branches of the fractal nanocrystals have been broken off owing to the fact that the sample in absolute alcohol is dispersed to TEM detection by ultrasonic vibration. The typical Fe_3O_4 fractal nanocrystal is displayed in Figure 4b. In the inset in Figure 4b is the high-magnification TEM image of the fractal branches. Close observation shows that each branch of the fractal has its own branch and grows forward along an identical direction. The phenomena are the same as the above SEM observations. The SAED and HRTEM images of the fractal nanocrystal are shown in Figure 4c. The SAED (inset in Figure 4c) obtained from the trunk part (marked by the ring in Figure 4b) of the fractal nanocrystal confirms the fractal nanocrystal to be crystalline. The HRTEM image obtained from the same place further supports the crystalline nature of the fractal nanocrystals. The interplanar spacing is about 0.481 nm, which corresponds to the (111) lattice planes. To further obtain the microstructure information of the junction of the trunk and branch, SAED and HRTEM also are used to detect the junction. Figure 5 exhibits SAED and HRTEM of the junction (marked by the ring in Figure 5a). The SAED shows that the junction almost possesses single-crystalline structure. Moreover, HRTEM also confirm the junction to be crystalline though the lattice fringes of HRTEM are not very clear in Figure 5b. The interplanar spacings are 0.294 and 0.481 nm, corresponding to (220) and (111) lattice planes, respectively. The results are consistent with SAED and HRTEM of the trunk mentioned above.

To understand the formation of the Fe_3O_4 nanocrystals, many experiments have been carried out. In the formation process of Fe_3O_4 fractals we find that PEG-20000 is necessary. If no PEG-20000 is added to the reaction system and keeping other conditions constant the products obtained are not the fractal nanocrystals but irregular large particles, which often appear as a collection of aggregated particles (not shown here). This indicates that initially formed magnetic Fe_3O_4 nanoparticles have a strong tendency to aggregate as larger ones when no protective agents are added. Thus, an appropriate amount PEG-20000 is very vital for the formation of Fe_3O_4 fractals. Although the exact roles of PEG-20000 on their growth are still unclear, it is believed that surfactant PEG-20000 might play a role for at least two aspects: preventing the aggregation of Fe_3O_4 nanoparticles in the initial stage and kinetically controlling the growth rates of various crystallographic facets of face-centered cubic Fe_3O_4 through selectively absorbing on these facets. The roles of PEG-20000 on the formation of the fractal nanocrystals are similar to these of poly(vinylpyrrolidone) (PVP) on the formation of Ag and Pb nanowires.[18] Besides PEG-20000, N_2H_4 plays an important role in the formation of Fe_3O_4. We cannot obtain pure Fe_3O_4 in the absence of the N_2H_4. This could be explained by the electrode potentials of the reactants; when comparing it is not difficult to find that N_2H_4 is able to oxidize Fe^{2+} in the ferrocene to Fe^{3+} in the reaction. Then Fe^{2+} and Fe^{3+} form Fe_3O_4. A similar reaction where N_2H_4 and Fe^{2+} serve as the oxidant and reductant, respectively, has been reported.[19] In addition, the temperature is also an important factor to the production of Fe_3O_4. If the reaction temperature is below 200 °C, we cannot obtain pure Fe_3O_4. On the other hand, if the temperature is too high, the reaction is difficult to control and sequentially the morphologies of Fe_3O_4 are not easy to selectively grow.

Now, we know about formation of the Fe_3O_4 fractal nanocrystals. However, how do the Fe_3O_4 fractal nanocrystals grow? As is well known, diffusion-limited aggregation (DLA) and nucleation-limited aggregation (NLA) models are usually used to interpret various fractals phenomena.[20] The microscopic nanocrystals anisotropy[21] and understanding the growth mechanism of side branching are very important to clarify the fractals formation. In our experiment surfactant PEG-20000 has the effect of kinetically controlling the anisotropy growth of the nanocrystals; this phenomenon has been discussed above. In addition, in numerous simulation and Hele−Shaw experiments[22] anisotropy has been found to be essential to produce stable tip behavior and repeated side branching of fractals. From another view, if the anisotropy growth of the material is strong, the growing interface of the fractals will be microscopically faceted, and the growth will possibly be governed by 2D nucleation, then it seems that we can also understand the side-branching phenomenon. Moreover, we assuredly obtain 2D-plane fractal nanocrystals. The oscillation of the concentration of the nanocrystals surface is another important factor to stable fractals formation.[21] This oscillation may be responsible for the periodic

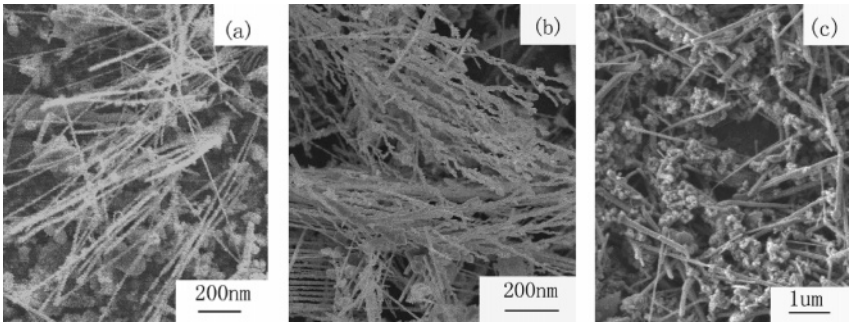

Figure 6. (a, b, and c) SEM images of the products when the ferrocene concentrations are 0.020, 0.042, and 0.10 mol/L, respectively.

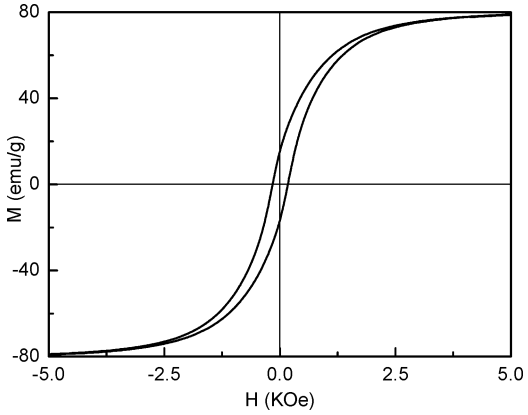

Figure 7. Magnetic hysteresis curves measured at room temperature for Fe_3O_4 fractal nanocrystals.

hesitation in fractals growth and the side-branching phenomenon.[23] In our experiments, because the reaction system proceeds in a sealed autoclave, which provides unstable and nonequilibrium experimental conditions, including the high reaction temperature and pressure, it was essential for producing the oscillating phenomena. Therefore, it cannot be ignored that the competition between the fractals growth and the solute transfer may become so evident under some circumstances that near the growing tip it will oscillate. Through the experiments we find that the concentration of ferrocene has a key influence on fractals growth, i.e., Fe^{2+} (that is ferrocene) transfer is related to the product morphology (i.e., fractals growth). When the ferrocene concentration (ca. 0.020 mol/L) is low in the reaction, only Fe_3O_4 nanowires and some nanoparticles can be produced (Figure 6a). With ferrocene concentration increasing and the Fe^{2+} concentration being enough to for anisotropy growth, side branching can occur. It is well known that large numbers of the branches grown on the fractals need more Fe^{2+}, and according to the above 2D nucleation, side branching can continually happen only if the reaction system has a relatively high concentration of starting materials. Thus, lots of fractals are obtained (Figure 6b) when the concentration of ferrocene is increased to ca. 0.042 mol/L. When further adding ferrocene to the reaction system, the products are almost invariable. However, an overfull quantity of ferocene is not favorable for the formation of fractal nanocrystals. For example, when the concentration of ferrocene reaches 0.10 mol/L, lots of Fe_3O_4 nanoparticles and some thick rods (Figure 6c) are produced. Accordingly, we find that the ferrocene concentration has a key effect on fractal formation. At the same time, it also indirectly confirms that oscillation of the concentration of the nanocrystals surface is an important factor to stable fractals formation.[21]

Figure 7 shows magnetic hysteresis curves for the samples measured at room temperature. The hysteresis loop of the Fe_3O_4 fractals exhibits a ferromagnetic behavior with saturation magnetization (M_s), remanent magnetization (M_r), and coercivity (H_c) values of ca. 78.750 emu/g, 15.22 emu/g, and 176.5 Oe, respectively; M_s of the products is different from the reported values (68.7 and 5.11 emu/g) of Fe_3O_4 nanowires.[15,17] Although the reasons are not clear, it is well known that the effects of size, structure, and morphologies are related to the magnetic properties of the products. Further work should be done to clarify the physical origin of the differences.

Conclusion

In summary, we facilely prepared novel fractals of magnetic Fe_3O_4 via a solvothermal process. There are three key factors, including ferrocene concentration, PEG-20000 role, and N_2H_4 as oxidant, discussed for formation of fractals. In particular, the ferrocene concentration has a key effect on the final morphologies of the products. The side-branching processes and oscillation of the concentration of the nanocrystals surface have been used to properly interpret formation of the fractals. The solvothermal and nonequilibrium process may be used to synthesize some other novel nanomaterials. In addition, the magnetic hysteresis measured shows that the fractals obtained display ferromagnetic properties at room temperature.

Acknowledgment. This work was supported by the National Natural Science Foundation of China and 973 Project of China. We appreciate Ms. Ying Wang from Lanzhou University for her friendly help in MS characterization.

References and Notes

(1) (a) Hu, J. T.; Odom, T. W.; Lieber, C. M. *Acc. Chem. Res.* **1999**, *32*, 435. (b) Alivisatos, A. P. *Science* **1996**, *271*, 933. (c) Ahmadi, J. S.; Wang, Z. L.; Green, T. C.; Henglein, A.; El-Sayed, M. A. *Science* **1996**, *272*, 1924. (d) Duan, X.; Huang, Y.; Cui, Y.; Wang, J.; Lieber, C. M. *Nature* **2001**, *409*, 66.

(2) (a) Zhang, Z.; Sun, X.; Dresselhaus, M. S.; Ying, J. Y. *Phys. Rev. B* **2000**, *61*, 4850. (b) Wang, Z. L. *Adv. Mater.* **2000**, *12*, 1295. (c) Cui, Y.; Wei, Q.; Park, H.; Lieber, C. M. *Science* **2001**, *293*, 1298.

(3) (a) Alivisatos, A. P. *J. Phys. Chem.* **1996**, *100*, 13226.

(4) (a) Iijima, S. *Nature* **1991**, *354*, 56. (b) Mayers, B.; Gates, B.; Yin, Y.; Xia, Y. *Adv. Mater.* **2001**, *13*, 1380. (c) Dykes, G. M.; Smith, D. K.; Seeley, G. J. *Angew. Chem., Int. Ed.* **2002**, *12*, 1148. (d) Xiao, J. P.; Xie, Y.; Tang, R.; Chen, M.; Tian, X. B. *Adv. Mater.* **2001**, *13*, 1887. (e) Huang, M. H.; Mao, S.; Feick, H.; Yan, H.; Wu, Y.; Kind, H.; Webber, E.; Russo, R.; Yang, P. *Science* **2001**, *292*, 1897. (f) Wang, X.; Li, Y. *J. Am. Chem. Soc.* **2002**, *124*, 2880. (g) Yuan, Z. Y.; Zhou, W. Z.; Su, B. L. *Chem. Commun.* **2002**, 1202. (h) Zhang, Y.; Suenaga, K.; Colliex, C.; Iijima, S. *Science* **1998**, *281*, 973. (i) Dai, Z. R.; Pan, Z. W.; Wang, Z. L. *J. Am. Chem. Soc.* **2002**, *124*, 8673.

(5) (a) Wan, W. M. V.; Greenham, N.; Friend, R. H. *J. Appl. Phys.* **2000**, *87*, 2542. (b) Cui, Y.; Lieber, C. M. *Science* **2001**, *291*, 851. (c) Cobden, D. H. *Nature* **2001**, *409*, 32.

(6) (a) Langer, J. S. *Rev. Mod. Phys.* **1980**, *52*, 1. (b) Ben-Jacob, E.; Garik, P. *Nature* **1990**, *343*, 523.

(7) (a) Wang, M.; Zhong, S.; Yin, X. B.; Zhu, J. M.; Peng, R. W.; Wang, Y.; Zhang, K. Q.; Ming, N. B. *Phys. Rev. Lett.* **2001**, *68*, 3827. (b) Wang, M.; Liu, X. Y.; Strom, C. S.; Bennema, P.; Enckevort, W.; Ming, N. B. *Phys. Rev. Lett.* **1998**, *80*, 3089.

(8) Peng, Q.; Dong, Y. J.; Deng, Z. X.; Li, Y. D. *Inorg. Chem.* **2002**, *41*, 5249.

(9) Kuang, D. B.; Xu, A. W.; Fang, Y. P.; Liu, H. Q.; Frommen, C.; Fenske, D. *Adv. Mater.* **2003**, *15*, 1747.

(10) (a) Goya, G. F.; Berquo, T. S.; Fonseca, F. C. *J. Appl. Phys.* **2003**, *94*, 3520. (b) Todorovic, M.; Schultz, S.; Wong, J.; Scherer, A. *Appl. Phys. Lett.* **1999**, *74*, 2516. (c) Zhang, X. J.; Jenekhe, S. A.; Perlstein, J. *Chem. Mater.* **1996**, *8*, 1571.

(11) Lepers, K. K. *Vestn. Akad. Nauk Kaz. SSR* **1990**, *4*, 26.

(12) Bate, G. In *Ferromagnetic Material*; Wohlfarth, E. D., Ed.; North-Holland: Amsterdam, 1980; Vol. 2 (Recording Materials), Chapter 7, p 381.

(13) Matijevic, P. E. In *Colloid Science of Composites System, Science of Ceramic Chemical Processing*; Hench, L. L., Ulrich, D. B., Eds.; Wiley: New York, 1986; p 463.

(14) (a) Darken, L. S.; Gurry, R. W. *J. Am. Chem. Soc.* **1946**, *68*, 798. (b) Osterhout, V. *Magnetic Oxides*; Wiley: New York, 1975; p 700. (c) Wang, S.; Xin, H.; Qian, Y. *Mater. Lett.* **1997**, *33*, 113. (d) Wang, C. Y.; Zhu, G. M.; Chen, Z. Y.; Lin, G. *Mater. Res. Bull.* **2002**, *37*, 2525. (e) Fan, R.; Chen, X. H.; Gui, Z.; Liu, L.; Chen, Z. Y. *Mater. Res. Bull.* **2001**, *36*, 497.

(15) Wang, J.; Chen, Q. W.; Zeng, C.; Hou, B. Y. *Adv. Mater.* **2004**, *16*, 137.

(16) Lian, S. Y.; Kang, Z. H.; Wang, E. B.; Jiang, M.; Hu, C. W.; Xu, L. *Solid State Commun.* **2003**, *127*, 605.

(17) Xu, L. Q.; Zhang, W. Q.; Ding, Y. W.; Peng, Y. Y.; Zhang, S. Y.; Yu, W. C.; Qian, Y. T. *J. Phys. Chem. B* **2004**, *108*, 10859.

(18) (a) Sun, Y. G.; Yin, Y. D.; Mayers, B.; Herricks, T.; Xia, Y. N. *Chem. Mater.* **2002**, *14*, 4736. (b) Wang, Y. L.; Herricks, T.; Xia, Y. N. *Nano Lett.* **2003**, *3*, 1163. (c) Sun, Y. G.; Gates, B.; Mayers, B.; Xia, Y. N. *Nano Lett.* **2002**, *2*, 165.

(19) (a) Wang, J.; Sun, J. J.; Sun, Q.; Chen, Q. W. *Mater. Res. Bull.* **2003**, *38*, 1113. (b) Xie, Y.; Zhu, L. Y.; Jiang, X. C.; Lu, J.; Zheng, X. W.; He, W.; Li, Y. Z. *Chem. Mater.* **2001**, *13*, 3927.

(20) (a) Halsey, T. C.; Duplantier, B.; Honda, K. *Phys. Rev. Lett.* **1997**, *78*, 1719. (b) Ming, N. B.; Wang, M.; Peng, R. W. *Phys. Rev. E* **1993**, *48*, 621.

(21) Wang, M.; Ming, N. B. *Phys. Rev. A* **1992**, *45*, 2493.

(22) (a) Kessler, D. A.; Koplik, J.; Levine, H. *Phys. Rev. A* **1984**, *30*, 2820. (b) Ben-Jacob, E. *Phys. Rev. Lett.* **1985**, *55*, 1315.

(23) Raz, E.; Lipson, S. G.; Polturak, E. *Phys. Rev. A* **1989**, *40*, 1088.